

A novel approach towards investigating the performance of different PVT configurations integrated on test cells: an experimental approach

Vivek Tomar^{a*}, G. N. Tiwari^a, Brian Norton^b

^aCentre for Energy Studies, Indian Institute of Technology (IIT) Delhi, New Delhi, 110016, India.

^bDublin Energy Lab, Dublin Institute of Technology (DIT), Dublin 7, Ireland.

Abstract

An analytical model of electrical and thermal performance for four different possible configuration of PVT integrated on identical test cells namely: (Glass-to-glass PV with duct integrated on a test cell, Glass-to-glass PV without duct integrated on a test cell (Glass to tedlar PV with duct integrated on a test cell and, Glass to tedlar PV without duct integrated on a test cell) has been developed and validated by experimental investigation in outdoor conditions. This glass to glass PV module give better both electrical thermal performance with hourly average η_m 12.65% and 12.70% for case 1 and 2 respectively. Similarly, hourly average η_{th} was observed 32.77% and 25.44% for case 1 and 2 respectively.

Keywords: Semi-transparent photovoltaic, Opaque photovoltaic, Electrical Efficiency, Solar radiation, Photovoltaic-thermal (PVT) system, Thermal energy, Test cell.

1. Introduction

Elevated photovoltaic (PV) cell operating temperature stimulate significant a reduction in open circuit voltage (V_{oc}) as well as accelerate light induced degradation of PV modules [1, 2]. Thus, the extraction of heat to reduce PV operating temperature leads to performance improvement in addition with proper arrangements it is possible to utilize the extracted thermal heat, Photovoltaic Thermal (PVT) system have been introduced [3]. Kern and Russel first one introduced the concept of PVT using air and water as a working fluid [4]. The monthly performance of photovoltaic increase from to 2.8% to 7.7% with of thermal efficiency about 49% by using an unglazed PVT configuration [5]. With introduction of metallic bond collector, and with water as a working fluid with single glazing increase PV electrical efficiency by 2% at a mass flow rate, 0.01kg/s [6]. A thermosyphon, PV integrated solar collector was designed for water heating applications. Dual heat extraction process has been developed for PVT energy system improvement and performance enhancement [7]. Integration of PV module over the air duct for composite climates enhances the overall thermal efficiency of collector due to utilization of extracted heat from PV module [8]. The various design of single and double pass air duct with glazed photovoltaic modules utilized as air heater for space heating and drying purpose has been developed and investigated [9,10, 11].

The performance of building as façade and roofs for both natural and forced circulation has been observed in experimentation with different PV technologies used [12, 13, 14]. Building integrated dual function solar collectors can be used in summer for space cooling [15]. Several electrical and thermal models for PVT air collector have been developed and have good agreement with the experimental results [16]. Recently, several study on opaque type building integrated PV roof, semitransparent PVT system used as a façade or in green-house have been conducted [17, 18]. In this study, two types of PV module, glass-to-glass and glass-to-tedlar, with two possible configurations with and without a duct are integrated on test cell. Four potential cases are studied in this research. Thermal model were developed to predict electrical and thermal efficiency of the PVT system in addition with potential solar heat gain of different configured PVT used as Building integrated PVT (BiPVT) system. Theoretical model were validated with experimental results performed in outdoor condition of New Delhi.

2. Thermal modelling and analysis of PV modules

In order to write the energy balance equation of photovoltaic modules, the following assumptions have been made:

- One-dimensional heat conduction ensues from exterior to interior of test cell.
- The glass cover is at a uniform temperature.
- The flow of air through the duct is considered stream line.
- The experiment was executed when the system is in quasi-steady state.
- The ohmic losses in the solar cell are considered negligible.
- Highly insulating material homogeneously configured inside test cells.
- Thermal loss due to ventilation/infiltration from the test cell are negligible.

Case 1: Glass to glass PV module with duct

For solar cells of PV module [1]

$$\alpha_c \beta_c \tau_g I(t) b dx = \left[U_{c,a} (T_c - T_a) + U_{c,f} (T_c - T_f) \right] b dx + \eta_c \tau_g \beta_c I_o b dx \quad (1)$$

$$\left[\begin{array}{c} \text{Available} \\ \text{solar energy rate} \\ \text{on solar cell} \end{array} \right] = \left[\begin{array}{c} \text{Overall heat} \\ \text{loss from top cell} \\ \text{surface to ambient} \end{array} \right] + \left[\begin{array}{c} \text{Heat transfer} \\ \text{rate from cell} \\ \text{to working fluid} \end{array} \right] + \left[\begin{array}{c} \text{Electrical} \\ \text{energy} \\ \text{production rate} \end{array} \right]$$

Where $U_{Gc,p} = U_{c,a} + U_{c,f}$ and $\eta_m = \eta_c \tau_g \beta_c$,

The values for design parameters as well as expression for different configuration are available in Table 1 and appendix respectively.

$$T_c = \left(\frac{U_{c,a}}{U_{Gc,p}} \right) T_a + \left(\frac{U_{c,f}}{U_{Gc,p}} \right) T_f + \left(\frac{\alpha_c \beta_c \tau_g I(t)}{U_{Gc,p}} \right) \left(1 - \frac{\eta_m}{\alpha \tau_{eff,1}} \right) \quad (1a)$$

The temperature dependent electrical efficiency of a PV module [1],

$$\eta_m = \eta_{mo} \left[1 - \beta_o (T_c - T_o) \right] \text{Where, } (T_c - T_o) \geq 0 \quad (2)$$

The operating temperature of cell using the temperature dependent electrical efficiency for PV module after substituting Eq. (2), the eq.(1) becomes,

$$T_c = \frac{\left(\frac{U_{c,a} T_a + U_{c,f} T_f}{U_{Gc,p}} \right) + \left(\frac{\alpha_c \beta_c \tau_g}{U_{Gc,p}} \right) I(t) - \left(\frac{\eta_{mo}}{U_{Gc,p}} \right) \{1 + \beta_o T_o\} I(t)}{\left(1 - \frac{\eta_{mo} \beta_o I(t)}{U_{Gc,p}} \right)} \quad (3a)$$

Nomenclature			
A	area (m ²)	U_{cf}	an overall heat transfer coefficient from solar cell to flowing air through glass cover/tehdar (W/m ² °C)
A_m	area of the PV module (m ²)	V_L	load voltage (V)
	width of PV module (m)	V_{oc}	open circuit voltage (V)
C_a	specific heat of air (J/kgK)	V, v	air velocity (m/sec)
DC	direct current	V_{max}	maximum voltage (V)
h	heat transfer coefficient (W/m ² oC)	V_{oc}	open circuit voltage (V)
h_o	heat transfer coefficient between a surface and ambient of account on convection and radiation (W/m ² oC)	<i>Subscripts</i>	
h_k	heat transfer coefficient through the glass cover of a solar cell (W/m ² oC)	a	ambient
h_r	radiative heat transfer coefficient ((W/m ² oC))	c	solar cell/module
h_{p1}	penalty factor due to presence of solar cell material, tedlar and EVA, dimensionless	eff	effective
h_{p2}	penalty factor due to presence of interface between tedlar and working fluid through absorber plate, dimensionless	f	working Fluid (air)
$I(t)$	incident solar intensity (W/m ²)	fi	inlet fluid
I_L	load current (A)	fo	outgoing fluid
I_{max}	maximum current in the module (A)	g, G	glass
I_{sc}	short circuit current in the module (A)	$G-G$	glass to Glass
K	thermal conductivity (W/m K)	ith	instantaneous Thermal
L	length of PV module (m)	oel	overall exergy
	mass flow rate (kg/sec)	oth	overall thermal
M	mass (kg)	p	blackened Plate
\dot{Q}_u	rate of useful energy transfer (W)	r	room (test cell inside)
t	time (s)	T	tedlar
\bar{T}	average temperature (°C or K)	th	thermal
T	temperature (°C or K)	<i>Greek letters</i>	
UL	overall heat transfer coefficient from solar cell to ambient through top and back surface of insulation (W/m ² °C)	α	absorptivity
$(UA)_T$	overall heat transfer coefficient from inside of test cell to ambient air temperature, (W/m ² °C)	$(\alpha\tau)_{eff}$	product of effective absorptivity and transmittivity
U_b	an overall back loss coefficient from flowing air/plate to ambient (W/m ² °C)	β	packing factor
$U_{p,a}$	an overall heat transfer coefficient from blackend plate to ambient through bottom surface (W/m ² °C)	β_o	temperature correction coefficient
U_L	an overall heat transfer coefficient for glass to glass and glass to tedlar modules (W/m ² °C)	τ	transmittivity
U_t	overall top loss coefficient of unglazed module (W/m ² °C)	η	efficiency
U_{Tt}	overall top loss coefficient of plate to ambient (W/m ² °C)	η_m	electrical efficiency of PV module
$U_{c,a}$	an overall heat transfer coefficient from solar cell to ambient through glass cover (W/m ² °C)	η_{mo}	efficiency at standard test condition (I(t) = 1000W/m ² and Ta = 25°C) (dimensionless)

The value of denominator term $(\eta_{mo}\beta_o I(t)/U_{Gc,p})$ has almost negligible value whatever the solar irradiance range 0-1000W/m².

Thus, $\left(1 - \frac{\eta_{mo}\beta_o I(t)}{U_{Gc,p}}\right) \cong 1$

$$T_c = \frac{(U_{c,a}T_a + U_{c,f}T_f)}{U_{Gc,p}} + \left\{ \frac{\alpha_c\beta_c\tau_g - \eta_{mo}(1 + \beta_o T_o)}{U_{Gc,p}} \right\} I(t) \quad (3)$$

For blackened absorber plate

$$[\alpha_p(1 - \beta_c)\tau_g I(t)]bdx = [h_f(T_p - T_f) + U_{p,a}(T_p - T_r)]bdx \quad (4)$$

$$\left[\begin{array}{l} \text{Solar energy rate} \\ \text{available on} \\ \text{blackened surface due} \\ \text{non packing area} \end{array} \right] = \left[\begin{array}{l} \text{Heat transfer} \\ \text{rate from blackened} \\ \text{plate to working fluid} \end{array} \right] + \left[\begin{array}{l} \text{Overall heat} \\ \text{loss from plate} \\ \text{to test cell} \end{array} \right]$$

From Eq. (4), the expression for plate temperature is given as,

$$T_p = \frac{\alpha\tau_{eff} I(t) + h_f T_f + U_{p,a} T_r}{U_{p,a} + h_f} \quad (4a)$$

For air flowing through the duct

$$\dot{m}_a C_a \frac{dT_f}{dx} = [h_f(T_p - T_f) + U_{c,f}(T_c - T_r)]bdx \quad (5)$$

$$\left[\begin{array}{l} \text{Mass flow} \\ \text{rate of flowing} \\ \text{fluid} \end{array} \right] = \left[\begin{array}{l} \text{Rate of heat} \\ \text{transfer from} \\ \text{blackened plate to} \\ \text{flowing fluid} \end{array} \right] + \left[\begin{array}{l} \text{Overall heat} \\ \text{transfer from cell} \\ \text{to test cell} \end{array} \right]$$

After substituting the eq. (3c) and (4a) in the eq. (5), the solution of first order differential equation with boundary condition, at $T_f|_{x=0} = T_{fi}$ and at $T_f|_{x=L} = T_{fo}$.

$$T_f|_{x=L} = \left[\frac{(\alpha\tau)_G I(t) + U_n T_r + U T_a}{U_{LG}} \right] \left[1 - \exp\left(-\frac{bU_{LG}L}{\dot{m}_a C_a}\right) \right] + T_f|_{x=0} \exp\left(-\frac{bU_{LG}L}{\dot{m}_a C_a}\right) \quad (5a)$$



Fig. 1. Photograph of the experimental set up at the roof-top of IIT Delhi, New Delhi.

The average air temperature over the air duct length below PV module is given as,

$$\bar{T}_f = \frac{1}{L} \int_0^L T_f dx = \left[\frac{(\alpha\tau)_G I(t) + U_b T_r + U_{c,a} T_a}{U_{L,G}} \right] \left[1 - \frac{1 - \exp\left(-\frac{bU_{L,G}L}{\dot{m}_a C_a}\right)}{\frac{bU_{L,G}L}{\dot{m}_a C_a}} \right] + T_p \frac{1 - \exp\left(-\frac{bU_{L,G}L}{\dot{m}_a C_a}\right)}{\frac{bU_{L,G}L}{\dot{m}_a C_a}} \quad (5b)$$

For test cell integrating ducted glass to glass PVT module

$$\dot{m}_a C_a (T_{f_0} - T_r) = M_r C_a \left(\frac{dT_r}{dt} \right) + (UA)_i (T_r - T_a) \quad (6)$$

After substituting the value of \bar{T}_f from eq.(5b), the solution of first order differential equation with boundary condition, at $T_r|_{t=0} = T_{ri}$ and at $T_r|_{t=t} = T_r = T_r$ is given as,

$$T_r = \frac{\bar{f}(t)}{a} (1 - e^{-at}) + T_{ri} e^{-at} \quad (7)$$

$$\text{Where, } a = \frac{1}{M_r C_a} \left[(UA)_i + \left(\frac{U_i}{U_i + U_{ri}} \right) \left\{ 1 - \exp\left(-\frac{bU_{L,G}L}{\dot{m}_a C_a}\right) \right\} \right],$$

$$\bar{f}(t) = \frac{1}{M_r C_a} \left[\dot{m}_a C_a \left(\frac{(\alpha\tau)_G I(t) + U_b T_r + U_{c,a} T_a}{U_i + U_{ri}} \right) \left\{ 1 - \exp\left(-\frac{bU_{L,G}L}{\dot{m}_a C_a}\right) \right\} + (UA)_i T_a \right]$$

If $T_{ri} = T_r$ and $T_f = \bar{T}_f$, then from Eqs. (2), (3c) and (5b), the expression for temperature dependent electrical efficiency is given as,

$$\eta_m = \eta_{mo} \left[1 - \beta_o \left\{ \left[\frac{(\alpha\tau)_{eff1} I(t) + U_{c,a} T_a}{U_{c,a} + U_{c,f}} \right] + \left[\frac{h_{p1} (\alpha\tau)_G I(t) + h_{p1} U_a T_r + h_{p1} U_{c,a} T_a}{U_{L,G}} \right] \right\} \right] \quad (8)$$

$$\text{where, } X_o = \frac{bU_{L,G}L}{\dot{m}_a C_a}$$

The hourly rate of useful thermal energy available at test cell after incorporated ducted glass to glass PVT module can be represented as,

$$\dot{Q}_u = M_r C_a \left(\frac{dT_r}{dt} \right) \quad (9)$$

Case 2: Glass to glass PV module without duct.

For solar cells of PV module [1]

$$\alpha_c \beta_c \tau_g I(t) b dx = [U_{c,a} (T_c - T_a) + U_b (T_c - T_r)] b dx + \eta_c \tau_g \beta_c I(t) b dx \quad (10)$$

$$\left[\begin{array}{l} \text{Available solar} \\ \text{energy rate} \\ \text{on PV module} \end{array} \right] = \left[\begin{array}{l} \text{Overall heat} \\ \text{loss from solar cell top} \\ \text{surface to ambient} \end{array} \right] + \left[\begin{array}{l} \text{Overall heat} \\ \text{loss from solar cell} \\ \text{back side to test cell} \end{array} \right] + \left[\begin{array}{l} \text{Electrical} \\ \text{energy production} \\ \text{rate} \end{array} \right]$$

Where, $\eta_m = \eta_c \tau_g \beta_c$. From Eq. (2), substituting the expression for temperature dependent electrical efficiency, after consider the approximation methods the expression for solar cell temperature become

$$T_c = \frac{(\alpha_c \beta_c \tau_g - \eta_{mo} (1 + \beta_o T_o)) I(t) + U_b T_r + U_{c,a} T_a}{U_{c,a} + U_b} \quad (10a)$$

For test cell integrating with glass to glass PV module

$$M_r C_a \frac{dT_r}{dt} + (UA)_i (T_r - T_a) = \tau_g (1 - \beta_c) I(t) A_m + U_b (T_c - T_r) A_m \quad (11)$$

After substituting the value of T_c from eq.(10a), the solution of first order differential equation with boundary condition, at $T_r|_{t=0} = T_{ri}$ and at $T_r|_{t=t} = T_r = T_r$ is given as,

$$T_r = \frac{\bar{f}(t)}{a} (1 - e^{-at}) + T_{ri} e^{-at} \quad (12)$$

$$\text{Where, } a = \left[\frac{(UA)_i + h_{b1} U_{c,a} A_m}{M_r C_a} \right], h_{b1} = \frac{U_b}{U_{c,a} + U_b}$$

$$f(t) = \left[\frac{\{\alpha\tau_{eff3} + \alpha\tau_{eff1} h_{b1}\} I(t) A_m + \{(UA)_i + h_{b1} U_{c,a} A_m\} T_a}{M_r C_a} \right]$$

The temperature dependent electrical efficiency of glass to glass PV module from Eq. (2), using Eqs. (12) and (10a) is given as,

$$\eta_m = \eta_{mo} \left[1 - \beta_o \left\{ \frac{\alpha\tau_{eff1} I(t) + U_b T_r + U_{c,a} T_a}{U_{c,a} + U_b} - T_o \right\} \right] \quad (13)$$

The hourly rate of useful thermal energy available in test cell installing glass to glass PV module can be represented as,

$$\dot{Q}_u = M_r C_a \left(\frac{dT_r}{dt} \right) \quad (14)$$

Case 3: Glass to tedlar PV module with duct

For solar cells of PV module [1]

$$[\alpha_s \beta_s + \alpha_r (1 - \beta_c)] I(t) b dx = [U_{c,a} (T_c - T_a) + U_T (T_c - T_p)] b dx + \tau_g \eta_c \beta_c I(t) b dx \quad (15)$$

$$\left[\begin{array}{l} \text{Solar energy} \\ \text{rate available} \\ \text{on PV module} \end{array} \right] = \left[\begin{array}{l} \text{Overall heat} \\ \text{loss from solar cell} \\ \text{top surface to ambient} \end{array} \right] + \left[\begin{array}{l} \text{Overall heat} \\ \text{transfer from solar cell} \\ \text{back surface to tedlar} \end{array} \right] + \left[\begin{array}{l} \text{Electrical} \\ \text{energy} \\ \text{production rate} \end{array} \right]$$

Where, $\eta_m = \eta_c \tau_g \beta_c$. After substituting Eq. (15) and using the approximation methods in Eq. (2),

$$T_c = \frac{U_{c,a} T_a + U_T T_p + [\tau_g \{\alpha_s \beta_s + \alpha_r (1 - \beta_c)\} - \eta_{mo} (1 + \beta_o T_o)] I(t)}{U_{c,a} + U_T} \quad (15a)$$

For the back surface of the tedlar

$$U_T (T_c - T_p) b dx = h_T (T_p - T_f) b dx \quad (16)$$

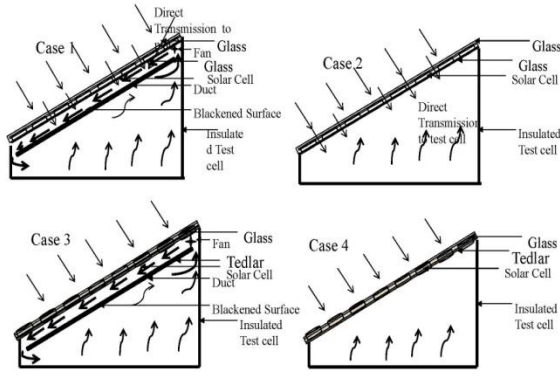


Fig. 2. Schematic view of four different possible configurations; (a) Case 1, (b) Case 2, (c) Case 3 and (d) Case 4.

$$\left[\begin{array}{c} \text{Overall heat transfer from} \\ \text{solar cell back surface to tedlar} \end{array} \right] = \left[\begin{array}{c} \text{Rate of heat transfer} \\ \text{from tedlar to working fluid} \end{array} \right]$$

After substituting Eq. (15a), the tedlar back surface temperature of PV module is given as,

$$T_p = \frac{h_{p1} \left[\tau_g \left\{ \alpha_c \beta_c + \alpha_f (1 - \beta_c) \right\} - \eta_{mo} (1 + \beta_o T_o) \right] I(t) + U_{tr} T_a + h_f T_f}{U_{n1} + h_f} \quad (16a)$$

For the air flowing below the tedlar

$$\dot{m}_a C_a \frac{dT_f}{dx} dx + U_{bb} (T_f - T_r) b dx = h_f (T_p - T_f) b dx \quad (17)$$

$$\left[\begin{array}{c} \text{Mass flow} \\ \text{rate of working} \\ \text{fluid} \end{array} \right] + \left[\begin{array}{c} \text{Overall heat transfer} \\ \text{from working fluid to} \\ \text{ambient} \end{array} \right] = \left[\begin{array}{c} \text{Rate of heat transfer} \\ \text{from tedlar back surface} \\ \text{to working fluid} \end{array} \right]$$

After substituting the eqs.(15a) and (16a) in the eq. (17), the solution of first order differential equation with boundary condition, at $T_f|_{x=0} = T_{fi} = T_{fi}$ and at $T_f|_{x=L} = T_{fo} = T_{fo}$.

$$T_f|_{x=L} = \left[\frac{h_{p2} h_{p1} \alpha_f \tau_g I(t) + U_{tr} T_a + U_{bb} T_r}{U_{L,T}} \right] \left[1 - \exp\left(-\frac{b U_{L,T} L}{\dot{m}_a C_a}\right) \right] + T_{fi} \exp\left(-\frac{b U_{L,T} L}{\dot{m}_a C_a}\right) \quad (17a)$$

The average air temperature over the air duct length below PV module is given as,

$$\bar{T}_f = \frac{1}{L} \int_0^L T_f dx = \left[\frac{h_{p2} h_{p1} \alpha_f \tau_g I(t) + U_{tr} T_a + U_{bb} T_r}{U_{L,T}} \right] \left[1 - \frac{1 - \exp\left(-\frac{b U_{L,T} L}{\dot{m}_a C_a}\right)}{\frac{b U_{L,T} L}{\dot{m}_a C_a}} \right] + T_{fi} \frac{1 - \exp\left(-\frac{b U_{L,T} L}{\dot{m}_a C_a}\right)}{\frac{b U_{L,T} L}{\dot{m}_a C_a}} \quad (17b)$$

For test cell integrating ducted glass to tedlar PVT module

$$\dot{m}_a C_a [T_{fo} - T_r] = M_r C_a \left(\frac{dT_r}{dt} \right) + (UA)_i (T_r - T_a) \quad (18)$$

After substituting the value of \bar{T}_f from eq.(17b), the solution of first order differential equation with boundary condition, at $T_r|_{t=0} = T_{ri} = T_{ri}$ and at $T_r|_{t=\tau} = T_{ro} = T_{ro}$ is given as,

$$T_r = \frac{\bar{f}(t)}{a} (1 - e^{-at}) + T_{ri} e^{-at} \quad (18a)$$

Where,

$$a = \frac{1}{M_r C_a} \left[(UA)_i + \left(\frac{U_{r,f}}{U_{L,T}} \right) \left\{ 1 - \exp\left(-\frac{b U_{L,T} L}{\dot{m}_a C_a}\right) \right\} \right]$$

$$f(t) = \frac{1}{M_r C_a} \left[\dot{m}_a C_a \left\{ \frac{h_{p2} h_{p1} \alpha_f \tau_g I(t) + U_{tr} T_a}{U_{L,T}} \right\} \left\{ 1 - \exp\left(-\frac{b U_{L,T} L}{\dot{m}_a C_a}\right) \right\} + (UA)_i T_a \right]$$

If $T_{fi} = T_r$ and $T_f = \bar{T}_f$, then from Eqs. (2), (15a) and (17b), the expression for temperature dependent electrical efficiency is given as,

$$\eta_m = \eta_{mo} \left[1 - \beta_o \left\{ \left(\frac{h_{p2} h_{p1} \alpha_f \tau_g I(t) + U_{tr} T_a + U_{bb} T_r}{U_{L,T}} \right) \left(1 - \frac{1 - \exp(-X_o)}{X_o} \right) \right\} + T_r \left(\frac{1 - \exp(-X_o)}{X_o} \right) \right] \left[\frac{U_{ca} T_a + \alpha_f \tau_g I(t) + h_{p1} h_{p2} \alpha_f \tau_g I(t) + h_{p1} U_{tr} T_a - T_o + \frac{h_{p1} h_f}{(U_{n1} + h_f)}}{U_{ca} + U_{tr}} + \frac{h_{p1} h_f}{(U_{n1} + h_f)} \right] \quad (19)$$

Where, $X_o = \frac{b U_{L,T} L}{\dot{m}_a C_a}$

The hourly rate of useful thermal energy obtained for a test cell after integrating glass to tedlar PVT module is given as,

$$\dot{Q}_u = M_r C_a \left(\frac{dT_r}{dt} \right) \quad (20)$$

Case 4: Glass to tedlar PV module without duct

For solar cells of PV module [1]

$$\tau_g [\alpha_c \beta_c + \alpha_f (1 - \beta_c)] I(t) b dx = [U_{ca} (T_c - T_a) + U_b (T_c - T_r)] b dx + \tau_g \eta \alpha_c \beta_c I(t) b dx \quad (21)$$

$\left[\begin{array}{c} \text{Solar energy} \\ \text{falling rate available} \\ \text{on PV module} \end{array} \right] = \left[\begin{array}{c} \text{Overall heat} \\ \text{loss from solar cell top} \\ \text{surface to ambient} \end{array} \right] + \left[\begin{array}{c} \text{Overall heat} \\ \text{loss from solar cell back} \\ \text{surface to test cell} \end{array} \right] + \left[\begin{array}{c} \text{Electrical} \\ \text{energy} \\ \text{production rate} \end{array} \right]$

Where, $\eta_m = \eta_c \tau_g \beta_c$. After substituting the Eq. (2), using expression for temperature dependent electrical efficiency in Eq. (21), using the approximation methods then expression for solar cell temperature is

$$T_c = \frac{\tau_g [\alpha_c \beta_c + \alpha_f (1 - \beta_c) - \eta_{mo} (1 + \beta_o T_o)] I(t) + U_{ca} T_a + U_b T_r}{(U_{ca} + U_b)} \quad (21a)$$

For test cell integrating glass to tedlar PV module

$$U_b (T_c - T_r) A_m = M_r C_a \left(\frac{dT_r}{dt} \right) + (UA)_i (T_r - T_a) \quad (22)$$

After substituting the value of T_c from eq.(21a), the solution of first order differential equation with boundary condition, at $T_r|_{t=0} = T_{ri} = T_{ri}$ and at $T_r|_{t=\tau} = T_{ro} = T_{ro}$ is given as,

$$T_r = \frac{\bar{f}(t)}{a} (1 - e^{-at}) + T_{ri} e^{-at} \quad (22a)$$

Where,

$$a = \left[\frac{(UA)_t + U_b(1-h_{p1})A_m}{M_r C_a} \right], h_{b1} = \frac{U_b}{(U_{t,c,a} + U_b)}$$

$$f(t) = \left[\frac{\alpha \tau_{eff} I(t) A_m h_{b1} + \{h_{b1} U_{c,a} A_m + (UA)_t\} T_a}{M_r C_a} \right]$$

The temperature dependent electrical efficiency Eqs (2) and (21a),

$$\eta_m = \eta_{mo} \left[1 - \beta_o \left\{ \frac{\alpha \tau_{eff} I(t) + U_{c,a} T_a + U_b T_r}{(U_{c,a} + U_b)} - T_o \right\} \right] \quad (23)$$

The rate of useful thermal energy obtained for a test cell after integrating glass to tedlar PV module is given as,

$$\dot{Q}_u = M_r C_a \left(\frac{dT_r}{dt} \right) \quad (24)$$

The electrical efficiency of PV can be calculated by the following expression [1],

$$\eta_m = \frac{I_{sc} \times V_{oc} \times FF - I_L \times V_L}{I(t) \times A_m} = \frac{I_m \times V_m - I_L \times V_L}{I(t) \times A_m} \quad (25)$$

Here, I_L and V_L are load current and voltage for a DC fan incorporated in ducted PV configuration of Case 1 and 3. FF is fill factor or power factor that defines the sharpness of I-V curve knee. The instantaneous thermal efficiency, η_{ith} have been calculated by using the following expression,

$$\eta_{ith} = \frac{\dot{Q}_u}{I(t) \times A_m} \quad (26)$$

The experimentally observed results are equating with the theoretical results used thermal modelling has been evaluated by considering two parameters; correlation coefficient, r and root mean square deviation, e measured by using following expression,

$$r = \frac{N \sum X_i Y_i - (\sum X_i)(\sum Y_i)}{\sqrt{N \sum X_i^2 - (\sum X_i)^2} \sqrt{N \sum Y_i^2 - (\sum Y_i)^2}} \quad (27)$$

- $r > 0$ indicates a positive linear relationship.
- $r < 0$ indicates a negative linear relationship.
- $r = 0$ implies no linear relationship between two variables.

$$\text{Root mean square percent deviation } e = \sqrt{\frac{\sum (e_i)^2}{N}} \quad (28)$$

where $e_i = \left[\frac{X_i - Y_i}{X_i} \right] \times 100$, Y_i (experimental values of variables),

and X_i (theoretical values of variables).

3. Experimental setup & system description

The experiment system consist of two types of mono-crystalline photovoltaic modules namely glass-to-glass and glass-to-tedlar with arrangement of duct and without duct integrated on prototype completely insulated identical test cells are considered in the study. The characteristic values of glass to glass PV and glass to tedlar PV modules as well as other parameters used to execute the experiment are tabulated in Table 1. The photographic view of all the two possible configurations of glass to glass PV module and glass to tedlar PV module with and without duct has been shown in Fig. 1. The schematic view of different configuration of glass to glass PV module for with and without a duct integrated on the test cell is shown in Fig.2 (a) & (b). Similarly, the arrangement of glass to tedlar PV module with duct and without a duct configuration integrated on test cell is depicted in Fig. 2 (c) & (d). For ducted cases, a DC of 12V is used to operate in forced mode, which is run by PV module directly. For this experiment, four prototype insulated identical test cell were fabricated and their design parameters used in the experimentation are tabulated in Table 2. In PVT with duct configuration, a DC fan is used to carry away

thermal energy available on back surface by blowing heated air from module to inside of test cell, this process is continuous go on without taking external air. During the experiment, inside air of test cell is continuously heating up over again and again.

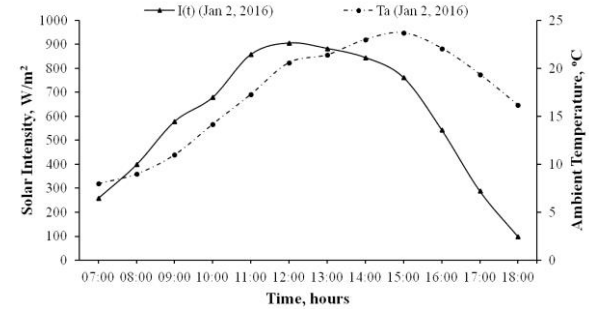


Fig. 3. The hourly variation of solar intensity, $I(t)$ and ambient temperature, T_a on the Jan 02, 2016.

The DC fan consume small amount of electricity and load current, I_L and load Voltage, V_L measured at regular interval, 60 min of time.

Table 1

Design parameters and characteristic values of both glass to tedlar and glass to glass PV modules used during the experiment

Parameter (Symbol)	Unit	Glass/tedlar PV	Glass/glass PV
b	m	0.66	0.69 m
L	m	0.8	1
m_a	kg/s	0.0058	0.0058
C_a	J/kg K	1005.00	1005.00
$U_{c,a}$	W/m² K	7.44	7.44
α_c	fraction	0.90	0.90
α_p	fraction	0.80	0.80
β_o	K-1	0.0045	0.0045
α_r	fraction	0.50	0.50
β_c	fraction	0.83	0.65
η_{mo}	fraction	0.13	0.135
τ_g	fraction	0.95	0.95
h_{p1}	fraction	0.898	0.536
h_{p2}	fraction	0.54	0.934
K_g	W/mK	1.1	1.1
L_g	m	0.003	0.003
K_T	W/mK	0.033	-
L_T	m	0.0005	-
U_b	W/m²K	3.36	3.23
$U_{c,f}$	W/m²K	-	8.59
$U_{L,G}$	W/m²K	4.42	4.56
P_{mp}	Watt	75	75
V_{mp}	Volt	17.5	17.7
I_{mp}	Ampere	4.14	4.2
V_{oc}	Volt	21	21.4
I_{sc}	Ampere	4.4	4.6

All the four PVT systems configurations are placed on the roof-top of a building situated at IIT Delhi Campus in New Delhi ([28°36'50"N 77°12'32"E](https://www.google.com/maps/place/28°36'50\)).

Table 2

Parameters of Test cell used in experimentation

Parameters	Units	Values
Inside wall surface (A_s)	m²	1.46
Inside volume of test cell	m³	0.56
Thickness of wood (l_w)	m	0.03
Mass of air inside test cell (M_r)	kg	0.686
Thickness of insulation (l_i)	m	0.15
Thermal conductivity of wood (k_w)	W/mK	0.09
Thermal conductivity of insulation (k_i)	W/mK	0.022

The photovoltaic parameters such as short-circuit current, I_{sc} , open circuit voltage, V_{oc} and maximum power, P_m and module electrical efficiency, ambient temperature, T_a and solar intensity, $I(t)$ were measured continuously with an interval of time, 60 min. To draw In

PVT configuration, PV modules were mounted on the prototype identical test cells in such a way that tilted angle of modules is equal to latitude of location with facing towards south as showed in photographic view of experimental setup Fig. 1. The current-voltage curve with fill factor, FF , maximum current, I_m and maximum voltage, V_m were measured for specific solar intensity at five different point of variable load, 0-5k Ω connected to modules.

4. Results & discussion

The hourly observed incident solar intensity, $I(t)$ on the PV modules and ambient temperature, T_a on Jan 02, 2016 is shown in Fig. 3. The solar irradiance attains maximum value 906W/m² in between around 12:00 to 13:00 and has maximum ambient temperature around 14:00 to 15:00 reached up to 23.7°C. This study have been carried to discuss all four cases; Case 1(Glass to glass PV module with duct instituted on test cell), Case 2(Glass to glass PV module without duct instituted on test cell), Case 3 (Glass to tedlar PV module with duct instituted on test cell) and Case 4 (Glass to tedlar PV module without duct instituted on test cell). Here in all cases, the used test cells are identical in shape and try to achieve complete insulation by diffusing insulating materials evenly. This study illustrates the benefits of Building integrated PV Thermal (BiPVT) system as well as helping the selection of the type suitable for a specific requirement based on climatic condition and load demands for space heating.

The variations of experimentally observed electrical efficiency for all the four cases using Eq. (25) has been shown in Fig. 4. The photovoltaic parameters measured for all cases have been measured at regular interval of time are tabulated in Table 3. The I_{sc} value for Case 1 and 2 does not shows much variance with installation of duct whereas even without duct (Case 2) have higher value as compared to without duct case (Case 1). These trends of I_{sc} for both cases are independent of weather conditions.

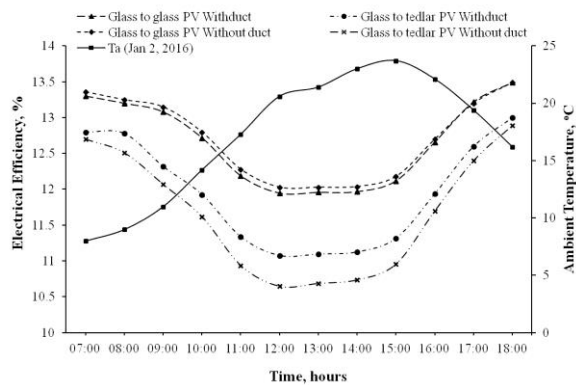


Fig. 4. The comparison of hourly observed electrical efficiency, η_m for different cases, and ambient temperature, T_a .

However, Cases 3 and 4 do not follow these trends, here installation of a duct enhances the performance of glass-to-tedlar PV module and likewise case 3 have higher I_{sc} as compared to case 4 as a lower operating temperature, T_c enhance PV module voltage; V_{oc} and cell current; I_{sc} . Moreover, an increase in I_{sc} has been observed with operating temperature reduction due to marginal increase of photo-generation rate along with reduction in band gap energy. The temperature rise enhances the dark current that induces negative effect on cell voltage due to rapid growth in reverse saturation current [31]. In glass to tedlar PV module, the open-circuit voltage, V_{oc} shows significant influenced of ducted case 3 than without ducted Case 4 due substantial decrease in module operating temperature, T_c of case 3. Since duct any how help to reduce the module temperature whereas on contrary glass to glass PV modules have not exhibited similar trends. Here, glass to glass PV module without duct (Case 2) have given higher V_{oc} as compared with ducted glass to glass PV module (Case 1) due to direct transmittance of incident solar irradiance through non packing area of module as well as absence of heated duct plate as encountered in

duct case. During this experiment the installation of a duct on test cell increased the room temperature; T_r (Test cell inside room temperature) for both kind of PV module; glass to glass and glass to tedlar.

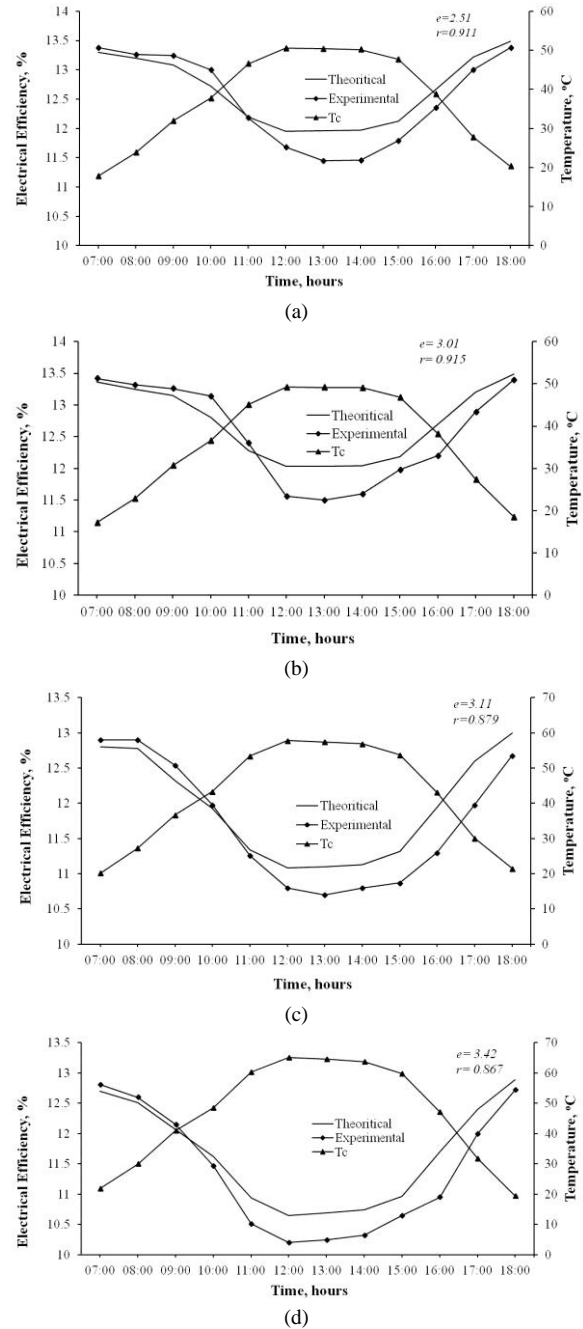


Fig. 5. The hourly variation of theoretical calculated and experimentally observed electrical efficiency, η_m and module temperature, T_c for different cases; (a) Case 1, (b) Case 2, (c) Case 3, and (d) Case 4.

Fig. 4 (a) compares the experimentally observed electrical efficiency at regular interval of time for different cases. After taking a close consideration, glass to glass PV module achieves higher efficiency compare to glass-to-tedlar PV module for both with and without duct cases. The glass-to-glass PV module achieved higher electrical efficiency as compared with glass to tedlar PV modules for all cases. Daily hourly average electrical efficiency for different cases has been found to be 12.7%, 12.7%, 11.9%, and 11.6% for Case 1, 2, 3 and 4 respectively. For Cases 1 and 2 (glass-to-glass PV), their electrical efficiency almost remain same. Variation in

efficiency was observed in Cases 3 and 4 (glass to tedlar PV). The theoretical electrical efficiency of glass to glass PV module for with and without duct has been calculated using Eqs. (8) and (13) respectively. Whereas, Eqs. (19) and (23) has been used to obtain theoretical electrical efficiency for glass to tedlar PV module with and without duct respectively.

The comparison of experimentally measured and hourly theoretically calculated electrical efficiency as well as measured PV module operating temperature, T_c for all the cases has been shown in Figs.5(a), (b), (c) and (d). Here, the calculated value also shows the variation with time first increase with time and decreases with time. The variation pattern of experimentally measured value followed exactly the same as followed by theoretical calculated values. The variation pattern of PV module electrical efficiency can be understood by module operating temperature fluctuation as temperature reaches up to maximum value their corresponding electrical efficiency approach to minimum value. Even with the incorporation of duct over both type of PV modules (glass to glass and glass to tedlar) the variation pattern remain same i.e. first decrease subsequently increase with time, their variation can be understood with operating temperature, T_c due to ambient temperature, T_a . The experimentally measured values have close agreement with theoretically calculated results. To equate theoretically calculated with experimentally observed results, Eqs. (27) and (28) were used to calculate correlation coefficient (r) and root mean square percent deviation (e) as depicted in Figs. 5. The maximum daily hourly average PV module operating temperature, T_c was attained by case 4 (Glass to tedlar PV module without duct)

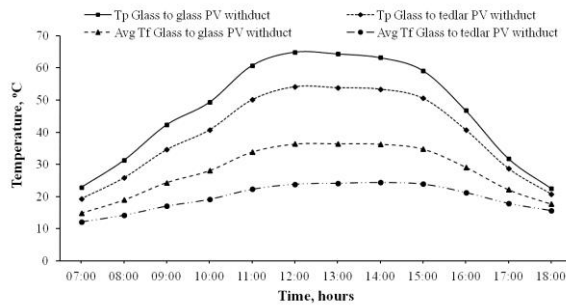


Fig. 6. The hourly variation of ducted blackened surface temperature and fluid temperature (average over the length of duct) for both Cases 1 and 3.

have value 46°C followed by 41.7°C of case 3 (Glass-to-tedlar PV module with duct) and their corresponding daily electrical average was about 11.65% and 11.95% respectively. For cases 1 and 2 (glass to glass PV module), daily average operating temperature of module, T_c was 36.7°C and 35.6°C in respectively. Similarly, their corresponding electrical efficiency, η_m does not show as much variation as shown by glass-to-tedlar PV modules (Cases 3 and 4) whereas case 2 (Glass-to-glass PV modules without duct) has little bit higher efficiency than case 1(Glass-to-glass PV module with duct). Thus, the duct helps to improve in electrical efficiency, η_m for both types of modules. For case 1 and 3, the ducted plate and fluid air temperature has been shown in Fig 6. Since the solar irradiance directly transmitted through the non-packing area of glass to glass PV module (Case 1), their blackened ducted plate get direct solar irradiance as well as conduction through solar cell where as in Case 3 (glass to tedlar) only conduction play dominant role. The daily average duct plate and fluid air temperature (average over the duct) of case 1 (glass to glass) was about 45°C and 27°C respectively. For case 3, daily average duct plate and average fluid (air) temperature over the duct (daily) was 37.2°C and 19°C respectively.

The comparison of instantaneous thermal efficiency for different cases in outdoor conditions has been depicted in Fig. 7. Generally, a PV module used to generate electrical energy but by using a proper

arrangement PV can also used for heat generation. For Cases 1 and 3, the main contribution in thermal energy using a duct integrated behind the PV module operate on a force mode that will help to increase inside air temperature by regular air circulation through the

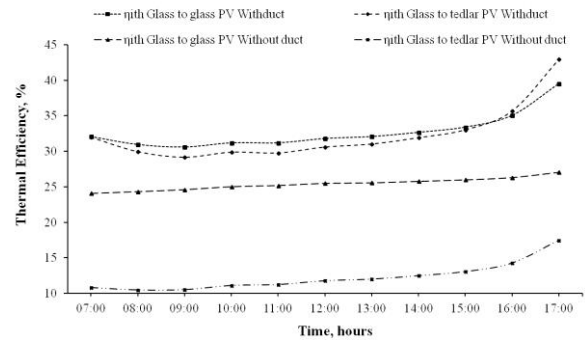


Fig. 7. The comparison of hourly measured instantaneous thermal efficiency, η_{ith} for different case.

duct. For Cases 2 and 4, thermal energy increases room temperature by direct transmission of solar irradiance passing through non packing area for glass-to-glass case along with conduction through solar cell for both glass-to-glass and glass-to-tedlar (in addition with conduction through tedlar). Eq. (26) is used to calculate instantaneous thermal efficiency. Instantaneous thermal efficiency represents how much heat is transferred to the test cell

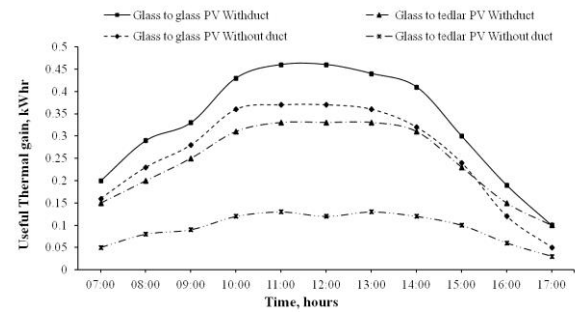


Fig. 8. Comparison of cumulative useful thermal gain obtained from different cases.

Hourly as thermal energy $M_r C_a (T_r - T_a)$ stored by increasing test cell air temperature with respect to available solar irradiance. Case 1 has maximum instantaneous thermal efficiency with daily average value 32.77% followed by case 3 with 32.37%. Moreover, Cases 2 and 4 does not show same trend and again case 2 shows better results with daily average value 25.40% of instantaneous thermal efficiency followed by 14.05% of case 4. In case of without duct, Case 2 shows better performance for thermal energy point of view. The hourly calculated thermal energy generated during experimentation for all the four cases has been given in Table 3. The useful thermal energy available for space heating in a day for all the four possible cases has been depicted in Fig. 8. The glass to glass PV with duct integrated test cell (Case 1) have maximum solar heat gain with an hourly average about 0.32kWhr as it has higher instantaneous thermal efficiency followed by Case 2 with value 0.24kWhr. Thus with increasing ambient temperature, T_a , the influence of duct become dominant and the performance of Case 3 become authoritative over Case 2.

It can be concluded from the above studies that glass to glass PV module have high capacity of heat dissipation even without duct (Case 2) its efficiency increases. The integration of duct will help to increase thermal efficiency for both types of PV modules and the unique combination of glass to glass PV with duct (Case 1) not only improves module electrical efficiency besides play an unparallel help in space heating for cold climatic condition. As ambient temperature, T_a becomes dominant over solar irradiance, the heat conduction through the non-packing area (tedlar) (Cases 3 and 4) plays important role as compared with solar irradiance transmission

for glass to glass case (Cases 1 and 2). Thus, it is inferred that Case 1 increases the room air temperature about 5°C in pursued by Case 2 with about 4°C change with respect to ambient temperature.

5. Conclusion

In this study, the performance of two types of PV (glass to glass and glass to tedlar PV modules) considering four possible configuration of PVT (Photovoltaic thermal modules) that employ the thermal aspects for building integrated applications of PV has been investigated and an analytical model has been developed for all the four cases. Experiment has been executed in an outdoor environment. A mathematical model has been experimentally validated. Agreement has been observed between experimentally observed and mathematically calculated values. The installation of duct behind glass-to-tedlar PV module helps decreases operating temperature, T_c with hourly average 5°C similarly for glass-to-glass PV module; it has reduced by an hourly average of 1.8°C. Since solar irradiance does not directly transmitted through duct and that enhances operating temperature of glass to glass PV modules. Whereas for both glass to glass PV and glass to tedlar PV, their electrical efficiency increases with an average 0.24% and 2.5% respectively. The glass-to-glass PV modules as compared with glass-to-tedlar PV module have higher electrical efficiency with an average of 0.9% for without duct and 1.20% for with duct case. From a thermal aspect, glass-to-glass PV with duct gives better performance with 2% higher in instantaneous thermal efficiency as compared glass-to-tedlar PV module with duct along with for glass to glass PV without duct have almost twice of instantaneous thermal efficiency as achieved by glass to tedlar without duct.

Appendix

In modelling equations, we used following relations for defining the design parameters, which are shown in Table 1.

(i) Case 1: Glass-to-glass PV module with duct

$$(\alpha\tau)_G = h_{p1}\alpha\tau_{eff1} + h_{p2}\alpha\tau_{eff2}$$

Here, $\alpha\tau_{eff1} = \alpha_c\beta_c\tau_g - \eta_{mo}(1 + \beta_oT_o)$ and $\alpha\tau_{eff2} = \alpha_p(1 - \beta_c)\tau_g$

h_{p1} and h_{p2} is the penalty factors due to glass cover of PV module,

which are defined as, $h_{p1} = \frac{U_{c,f}}{U_{c,a} + U_{c,f}}$ and $h_{p2} = \frac{h_f}{U_{p,a} + h_f}$

$$U_{c,a} = \left[\frac{L_g}{K_g} + \frac{1}{h_o} \right]^{-1}, h_o = 5.7 + 3.8V, V = 1m/s$$

$$U_{c,f} = \left[\frac{L_g}{K_g} + \frac{1}{h_i} \right]^{-1}, h_i = 2.8 + 3v, v = 2m/s$$

$$U_t = \frac{U_{c,f} \cdot U_{c,a}}{U_{c,f} + U_{c,a}}, U_{Ti} = \frac{U_{p,a} \cdot h_f}{U_{p,a} + h_f}, U_{L,G} = U_t + U_{Ti}$$

(ii) Case 2: Glass-to-glass PV module without duct

$$\alpha\tau_{eff1} = \alpha_c\beta_c\tau_g - \eta_{mo}(1 + \beta_oT_o), \alpha\tau_{eff3} = \tau_g(1 - \beta_c)$$

$$U_{c,a} = \left[\frac{L_g}{K_g} + \frac{1}{h_o} \right]^{-1}, h_o = 5.7 + 3.8V, V = 1m/s$$

$$U_b = \left[\frac{L_g}{K_g} + \frac{1}{h_i} \right]^{-1}, h_i = 2.8 + 3v, v = 0m/s$$

(iii) Case 3: Glass-to-tedlar PV module with duct

$$\alpha\tau_{eff} = [\tau_g \{ \alpha_c\beta_c + \alpha_p(1 - \beta_c) \} - \eta_{mo}(1 + \beta_oT_o)]$$

h_{p1} and h_{p2} is the penalty factors due to glass cover and tedlar of PV module, which are defined as,

$$h_{p1} = \frac{U_T}{U_{c,a} + U_T} \text{ and } h_{p2} = \frac{h_T}{U_{c,a} + h_T}$$

$$U_{c,a} = \left[\frac{L_g}{K_g} + \frac{1}{h_o} \right]^{-1}, h_o = 5.7 + 3.8V, V = 1m/s$$

$$U_T = \left[\frac{L_T}{K_T} + \frac{1}{h_T} \right]^{-1}, h_T = 2.8 + 3v, v = 2m/s$$

$$U_{Ti} = \frac{U_{c,a} \cdot U_T}{U_{c,a} + U_T}, U_{i,f} = \frac{U_{\alpha} \cdot h_T}{U_{i,f} + h_T}, U_{L,T} = U_{i,f} + U_{Ti}$$

(iv) Case 4: Glass-to-tedlar PV module without duct

$$\alpha\tau_{eff} = \tau_g [\alpha_c\beta_c + \alpha_p(1 - \beta_c) - \eta_{mo}(1 + \beta_oT_o)]$$

$$U_{c,a} = \left[\frac{L_g}{K_g} + \frac{1}{h_o} \right]^{-1}, h_o = 5.7 + 3.8V, V = 1m/s$$

$$U_b = \left[\frac{L_T}{K_T} + \frac{1}{h_i} \right]^{-1}, h_i = 2.8 + 3v, v = 0m/s$$

References

- [1] Tiwari GN, Mishra RK, Solanki SC. Photovoltaic modules and their applications: a review on thermal modelling. Applied Energy 2001;88:2287–2304.
- [2] Norton, B., Philip, C., Tapas, K.M., Huang, M.J., McCormack, S.J., Mondol, J.D., Yigzaw, G.Y., 2010. Enhancing the performance of building integrated photovoltaics. Solar Energy 85, 1629–1664.
- [3] Odeh N, Grassie T, Henderson D, Muneer T. Modelling of flow rate in a photovoltaic-driven roof slate-based solar ventilation air pre heating system, Energy Conversion Management 2006;47:909–925.
- [4] Kern Jr EC, Russell MC. Combined photovoltaic and thermal hybrid collector systems. In: Proceedings of the 13th IEEE photovoltaic specialists. Washington, DC, USA; 1978. p. 1153–7.
- [5] Kalogirou SA. Use of TRYNYSYS for modeling and simulation of a hybrid PV-thermal solar system for Cyprus, Renewable Energy 2001;23:247–260.
- [6] Chow TT. Performance analysis of photovoltaic-thermal collector by explicit dynamic model, Solar Energy 2003;75:143–152.
- [7] Tripanagnostopoulos Y. Aspects and improvements of hybrid photovoltaic/ thermal solar energy systems. Sol energy 2007;81:1117–31.
- [8] Tiwari A, Sodha MS, Chandra A, Joshi JC. Performance evaluation of photovoltaic thermal solar air collector for composite climate of India, Solar Energy Materials and Cells 2006;90:175–189.
- [9] Huang BJ, Lin TH, Hung WC, Sun FS. Performance evaluation of solar photovoltaic/thermal systems, Solar Energy 2001;70: 443–448.
- [10] Sopian K, Liu HT, Kakac S, Veziroglu TN. Performance of a double pass photovoltaic thermal solar collector suitable for solar drying systems, Energy Conversion and Management 2000;41:353–365.
- [11] Tonui JK, Tripanagnostopoulos Y. Performance improvement of PV/T solar collectors with natural air flow operation. Solar Energy 2008;82:1–12.

- [12] Zondag HA, de Vries DW, van Helden WGJ, van Zolingen RJC, van Steenhoven AA. The thermal and electrical yield of a PV-thermal collector, *Solar Energy* 2002;72:113–128.
- [13] Abu-Bakar SH, Muhammad-Sukki F, Freier D, Ramirez-Iniguez R, Mallick TK, Munir AB, et al. Performance analysis of a novel rotationally asymmetrical compound parabolic concentrator. *Appl Energy* 2015;154:221–31.
- [14] Hu J, Chen W, Yang D, Zhao B, Song H, Ge B. Energy performance of ETFE cushion roof integrated photovoltaic/thermal system on hot and cold days. *Appl Energy* 2016;173: 40–51.
- [15] Ji J, Luo C, Chow TT, Sun W, He W. Thermal characteristics of a building integrated dual-function solar collector in water heating mode with natural circulation. *Energy* 2011;36:566–74.
- [16] He W, Chow TT, Ji J, Lu J, Pei G, Chan L. Hybrid photovoltaic and thermal solar collector designed for natural circulation of water. *Appl Energy* 2006;83:199–210.
- [17] Agrawal B, Tiwari GN. Optimizing the energy and exergy of building integrated photovoltaic thermal (BIPVT) systems under cold climatic conditions. *Appl Energy* 2010;87:417–26.
- [18] Kamthania D, Nayak S, Tiwari GN. Performance evaluation of a hybrid photovoltaic thermal double pass facade for space heating. *Energy Build* 2011;43(9):2274–81.

Table 3

Hourly variation of I_{sc} , V_{oc} , FF and η_m , of four PV configurations; (a) glass to glass PV modules with and without duct in winter. (b) glass to tedlar PV modules with and without duct have also been given.

Time (hr)	I_{sc} (A)		V_{oc} (V)		FF		η_m (%)		T_r (°C)		P_m (W)		Thermal Energy (W)	
	With duct	Without duct	With duct	Without duct	With duct	Without duct	With duct	Without duct	With duct	Without duct	With duct	Without duct	With duct	Without duct
07:00	2.00	2.18	20.78	20.82	0.57	0.52	13.3	13.36	8.2	8.1	23.61	23.62	66.69	40.71
08:00	3.00	3.16	20.60	20.72	0.57	0.54	13.2	13.25	9.5	9.4	35.43	35.44	99.03	63.31
09:00	3.72	3.74	19.61	19.71	0.68	0.67	13.08	13.15	11.9	11.7	49.61	49.6	141.95	92.87
10:00	3.98	4.00	19.50	19.69	0.73	0.72	12.72	12.8	15.6	15.3	56.71	56.63	169.76	110.85
11:00	4.38	4.40	19.10	19.38	0.82	0.80	12.19	12.28	19.3	18.9	68.75	68.59	214.34	140.93
12:00	4.46	4.47	18.60	18.87	0.86	0.84	11.95	12.03	23.3	22.8	71.19	70.94	230.66	150.60
13:00	4.40	4.42	18.70	18.77	0.84	0.83	11.96	12.03	24.7	24.1	69.4	69.18	226.72	147.26
14:00	4.31	4.32	19.03	19.07	0.81	0.80	11.97	12.04	27	26.2	66.47	66.25	221.08	142.21
15:00	4.12	4.13	19.40	19.37	0.76	0.76	12.12	12.18	28.3	27.4	60.64	60.45	203.88	129.42
16:00	3.55	3.57	19.83	19.85	0.64	0.64	12.66	12.7	27.1	26.1	45.14	45.06	152.89	93.81
17:00	2.00	2.67	20.12	20.17	0.63	0.47	13.22	13.2	24.7	23.6	25.2	25.2	91.73	51.58
18:00	1.40	1.47	9.6	9.40	0.93	0.66	13.49	13.49	21.6	20.5	12.56	9.04	52.68	19.28

(a)

Time (hr)	I_{sc} (A)		V_{oc} (V)		FF		η_m (%)		T_r (°C)		P_m (W)		Thermal Energy (W)	
	With duct	Without duct	With duct	Without duct	With duct	Without duct	With duct	Without duct	With duct	Without duct	With duct	Without duct	With duct	Without duct
07:00	1.80	1.79	19.28	19.10	0.60	0.61	12.8	12.7	8.1	8	20.89	20.74	50.33	17.01
08:00	2.54	2.49	19.00	18.51	0.64	0.67	12.78	12.51	9.4	9.1	31.14	30.76	72.51	25.38
09:00	3.47	3.36	18.76	18.36	0.66	0.69	12.32	12.07	11.7	11.2	43.21	42.35	102.41	36.94
10:00	3.69	3.56	18.25	17.73	0.73	0.76	11.93	11.62	15.2	14.6	49.12	47.86	123.07	45.76
11:00	4.15	3.91	17.82	17.22	0.80	0.84	11.34	10.94	18.8	17.8	58.93	56.87	154.83	58.48
12:00	4.21	4.05	17.35	16.77	0.83	0.86	11.08	10.65	22.5	21.3	60.81	58.45	167.90	64.62
13:00	4.16	4.01	17.42	16.78	0.82	0.85	11.1	10.69	23.8	22.3	59.37	57.16	165.90	64.22
14:00	4.01	3.87	17.92	17.35	0.79	0.82	11.13	10.74	25.9	24.1	56.99	54.96	163.40	63.96
15:00	3.81	3.69	18.62	18.28	0.74	0.75	11.32	10.96	27	25	52.24	50.61	152.54	60.34
16:00	3.27	3.20	19.26	18.87	0.63	0.64	11.94	11.7	25.8	23.5	39.38	38.6	117.71	47.10
17:00	1.67	1.56	18.51	18.22	0.72	0.78	12.6	12.4	23.3	20.9	22.29	22.11	75.36	30.69
18:00	1.36	1.12	18.30	18.15	0.45	0.40	13	12.89	20.2	17.7	11.19	8.06	47.36	17.11

(b)